



# A Numerical Study Of The Effect Of The Compression Ratio On The Biodiesel Fuel Spray Characteristics At Different Blending Ratios.

Nourhan Hesham, Mostafa Abdelkhalek, Ashraf Mostafa, M. Kamal,

Mechanical Power Engineering Department, Faculty of Engineering, Ain Shams University, Cairo, Egypt

## Abstract

In this paper a Computational fluid dynamic study was done to investigate the effect of different compression ratios and different biodiesel blending ratios on the spray characteristics. A three dimensional numerical simulation was done using ANSYS-FLUENT by using internal combustion engine module. This simulation was done on a 4-stroke engine for a Ruggerini RD 270 engine. A cold flow simulation was carried for the engine with compression ratio 18 and it was validated against [1] that was validated experimentally against a compression test performed on the engine at the "Green Energy Lab" at Faculty of Engineering, Ain Shams University. Another two cold flow simulations for compression ratios 17 and 16 were done upon this validation. After that a diesel spray model was integrated to the cold flow engine with compression ratio 18 and it was validated against [1] by comparing the penetrating length for the two models. Upon that a spray models for Diesel and different Biodiesel blending ratios 20% , 60% and 100 % were integrated to the three compression ratio engines 18 , 17 , and 16 respectively to study the effect of different compression ratios and the different biodiesel blending ratios on spray penetrating length .

**Key words:** CFD, Biodiesel, Penetrating length, Compression ratio.

## 1. Introduction

Due to the great importance to find an alternative fuel for diesel to achieve clean energy production, many studies were carried to study the effect of different parameters on spray characteristics such as spray penetrating length to improve the quality of the combustion process. As the characteristics and the atomization process of the fuel spray has a big effect on soot emissions and combustion efficiency. Experimental and numerical study was carried by [2] to study the effect of biodiesel blending ratios and the injection pressure on spray characteristics, and it was showed that the spray behavior changed according to any change in density and surface tension of the fuel, also any change in the injection pressure has a great effect on the spray behavior. Numerical study was carried by [3] to study the effect of the ambient back pressure and temperature on fuel spray behavior and it was found that increasing the ambient temperature caused the penetrating length to increase at all different back pressure. A numerical study was done by [4] to study the biodiesel spray behavior and it was shown that biodiesel spray has the same behavior trend as diesel except it showed lower values when it compared to diesel because biodiesel has higher density. Results stated by [5] showed that as the injection pressure increased the spray penetration length of diesel and biodiesel increased, and it also showed that the spray angle become wider. Another study [6] showed that increasing injection pressure caused the spray tip

penetration to increase, and increasing the biodiesel blending ratio resulted in decreasing the spray tip penetration compared to diesel .Due to the importance of this field, this paper studied the effect of different compression ratios 18, 17, 16 and the effect of Diesel and of different biodiesel ratios 20 %, 60 %, 100 % on spray penetrating length.

## 2. Numerical Setup:

### ENGINE MODEL

**Table1: Ruggerini RD 270 engine specifications.**

Number of cylinders	2
Cooling	Air cooled
Bore	95 mm
Stroke	85 mm
Swept volume	1205 cc
Compression ratio	18:1
Clearance	4.7 mm
Connecting rod	187 mm
Crank radius	42.5 mm
Injector hole diameter	0.28 mm
Rated power	20 kW (27.2 Hp) @ 3000 rpm

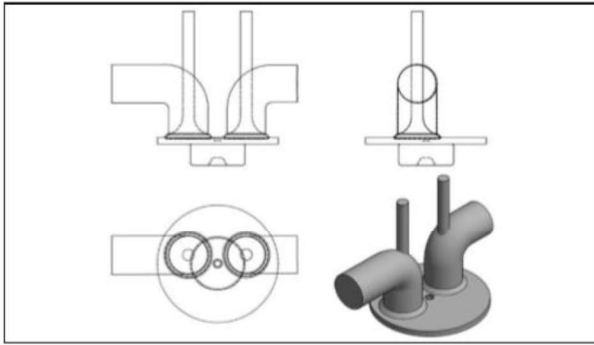


Figure 1: Engine geometry using Inventor-CAD.

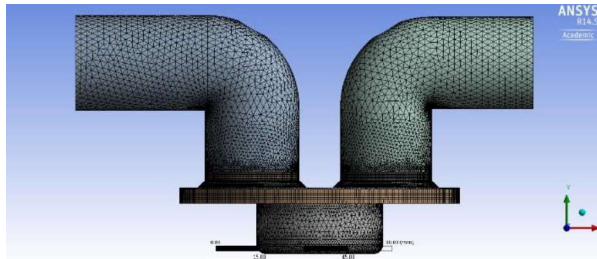


Figure 2: Meshing process.

A three dimensional geometry was designed using Inventor-CAD as shown in Figure 1, and it was imported by Internal Combustion Engine module in Ansys-Fluent then it was decomposed and meshed as shown in Figure 2. A cold flow simulation was carried in this model with model specifications as shown in Table 1 where only the air motion was simulated without taking any chemical characteristics into consideration.

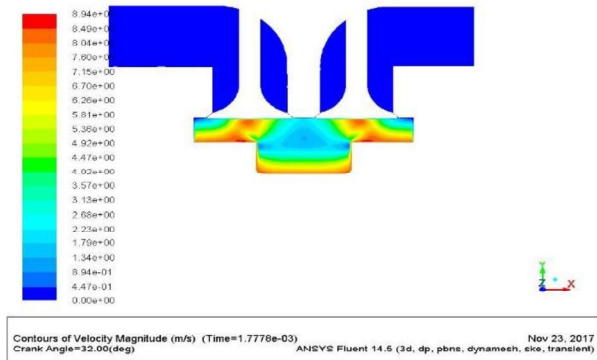


Figure 3: Velocity contour.

Figure 3 showed the velocity contour obtained from the cold flow simulation of the engine at crank angle 32°. The simulation was done for 5 periodic cycles (5x4 strokes) to remove any initial transients.

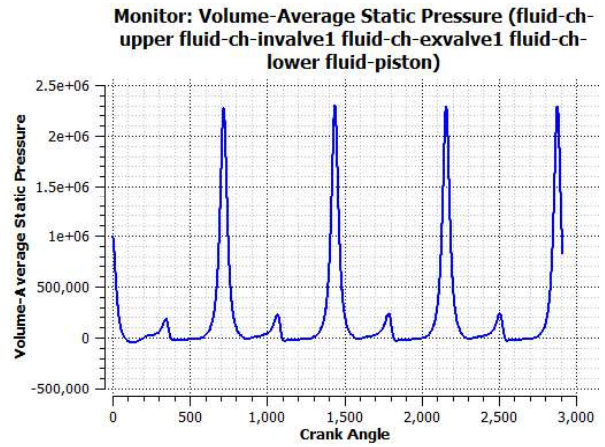


Figure 4: Cylinder pressure in Pascal vs. Crank angles in degree.

The maximum pressure as shown in Figure 4 is 23 bar which is validated against the result stated by [1] and it showed an agreement with it.

**GRID INDEPENDENCE STUDY**

This test was carried with two different mesh resolution with the following specifications as shown in Table 2. The mesh cells that is used here is Tetrahedron cells as shown in Figure 2. The result of the fine mesh resolution is the peak pressure of 23 bar as shown in Figure 4, and the result of the peak pressure of the coarse mesh resolution is also 23 bar as shown in Figure 5.

Table 2: Grid independency study.

M mesh resolution	fine	coarse
Number of Tetrahedron Elements	221012	60825
N Number of nodes	1062219	330791

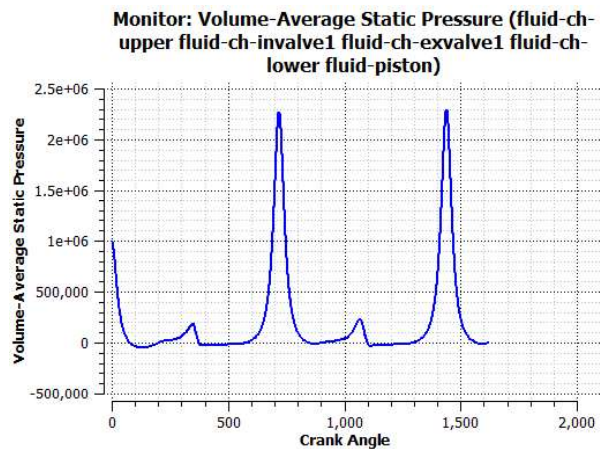


Figure 5: pressure in Pascal vs. crank angle in degree for coarse mesh resolution.

After the engine model with compression ratio 18 was validated against [1] and after the agreement with the two mesh resolution another two cold flow engine models were done for compression ratio 17 and 16. The results of the peak pressure for compression ratios

17 and 16 are 22 bar and 21 bar respectively as shown in Figure 6 and 7 respectively.

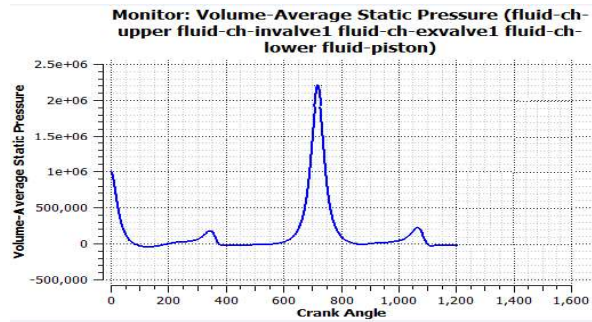


Figure 6: pressure in Pascal vs. crank angle in degree for engine with compression ratio 17.

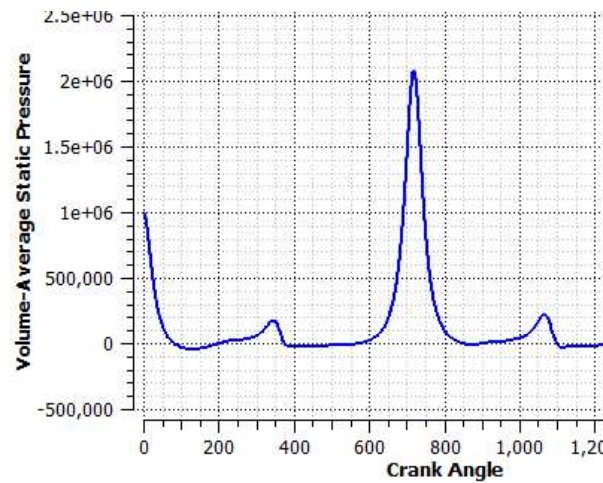


Figure 7: pressure in Pascal vs. crank angle in degree for engine with compression ratio 16.

**SPRAY MODEL**

The dispersed phase model was activated to simulate the spray model. The dispersed phase model solve continuous phase with the Eulerian approach and it uses the lagrangian approach to track the spray particles.

It was recommended by [1] to activate the coupling option between the continuous phase and the spray. The Kelvin-Helmholtz Rayleigh-Taylor (KH-RT) model was activated as it was recommended by [1].the spray model is integrated to engine model with the compression ratio 18.

**Table 3: spray system specifications.**

Diesel density	830 $\frac{kg}{m^3}$
Diesel kinematic viscosity	3.5 $\frac{mm^2}{s}$
Biodiesel density	880 $\frac{kg}{m^3}$
Biodiesel kinematic viscosity	5.21 $\frac{mm^2}{s}$
Nozzle diameter	0.00028 m
Nozzle length	0.00056 m
Injection pressure	350 bar
Injection mass flow rate	0.008738 kg/s.

Diesel fuel with density and kinematic viscosity as shown in Table 3 was used. The diesel was injected by four holes with specifications shown in Table 3. The resulted penetrating length was validated against penetrating length obtained by [1], and it showed an agreement as shown in Figure 8 but with a small deviation that may be due to the accuracy of the measurement software tool that differ from Ansys version to another. After validating the diesel spray model with the engine with compression ratio 18 another simulation was done with the diesel spray with the engine models with compression ratio 17 and 16. Also, other simulations were carried for different biodiesel blending ratios 20%, 60% and 100% and were integrated to engine models with compression ratio 18, 17 and 16 respectively. The biodiesel used is of density and of kinematic viscosity as shown in Table 3.

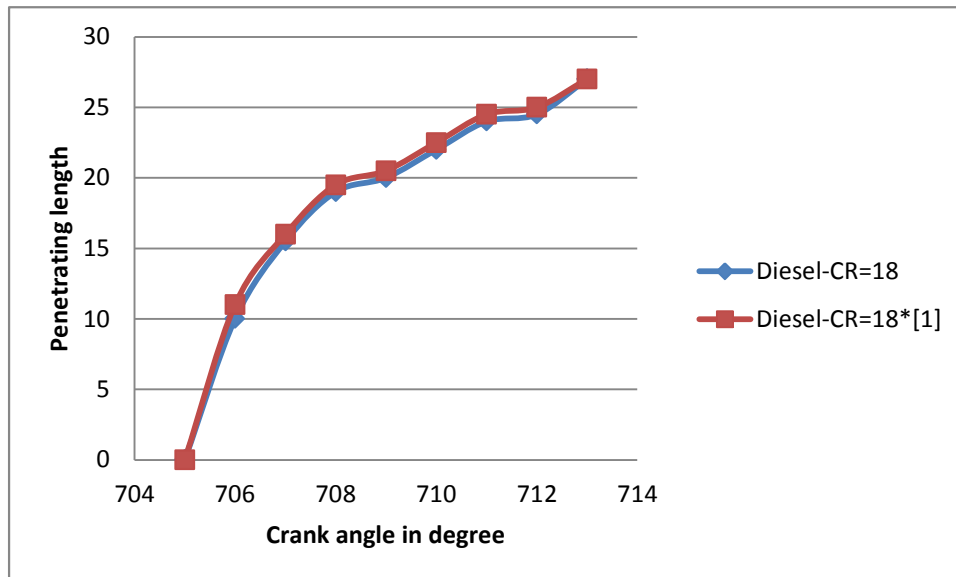


Figure 8: penetrating length of diesel spray of current study vs. the penetrating length obtained by study [1] at compression ratio CR= 18.

### 3. Results and discussion

Figure 9 shows that as the compression ratio increases the spray penetrating length decreases that is because of the higher pressure caused by increasing the compression ratio that made the spray to break up faster .

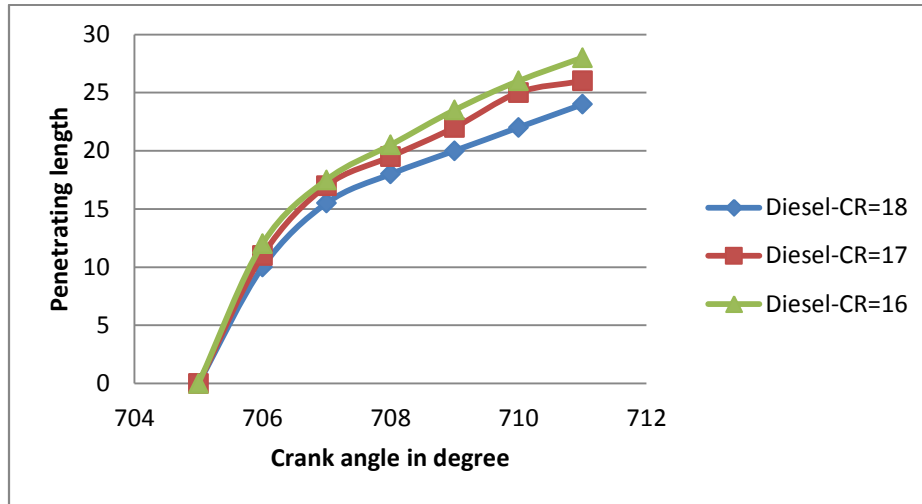


Figure 9: penetration length of diesel spray at different compression ratio.

Figure 10, 11 and 12 showed that during compression ratio 18, 17, and 16 respectively as the biodiesel blending ratio increased the spray penetrating length increased that is because increasing the blending ratio caused increasing the viscosity which caused higher particle momentum causing longer penetrating length.

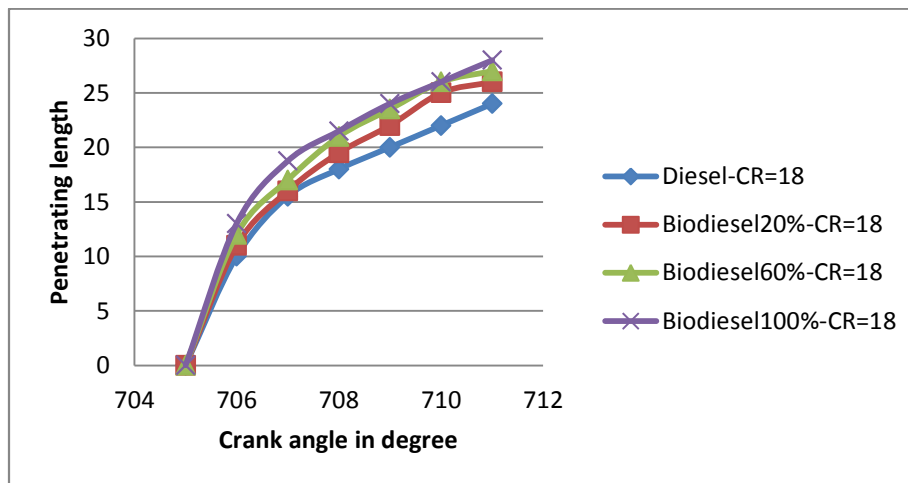


Figure 10: penetrating length of different biodiesel blending ratios at compression ratio CR= 18.

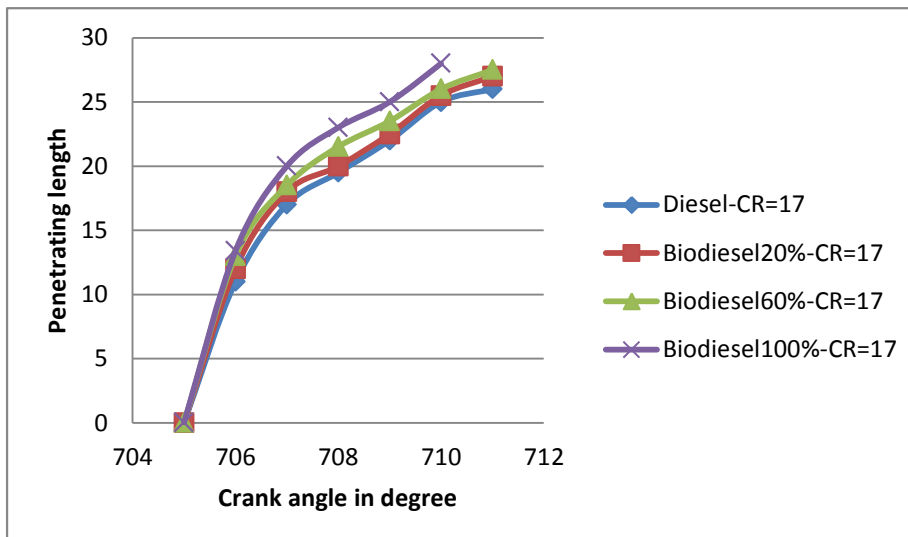


Figure 11: penetrating length of different biodiesel blending ratios at compression ratio CR= 17.

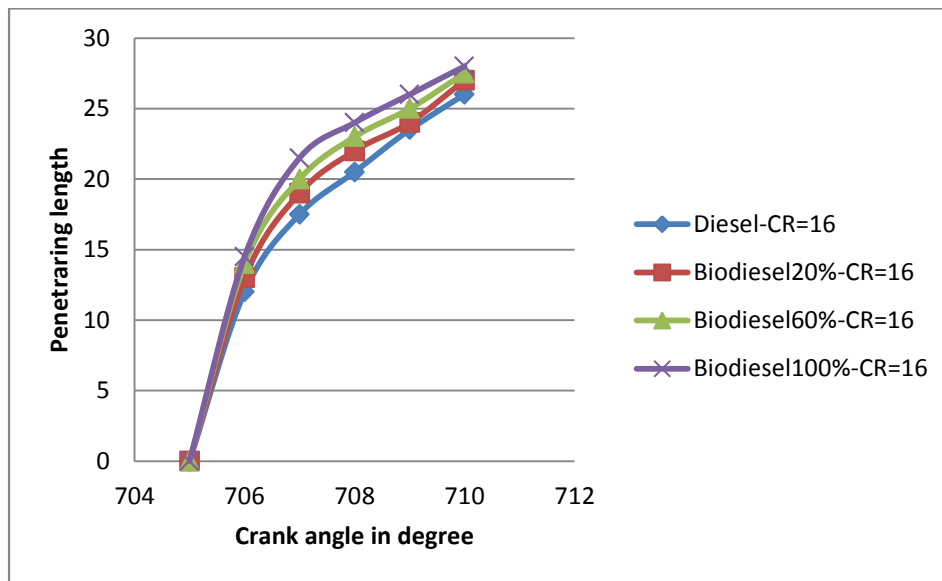


Figure 12: penetrating length of different biodiesel blending ratios at compression ratio CR= 16.

Figure 13 showed that during biodiesel blending ratio 100% as the compression ratio increases the spray penetrating length decreases that is because of the higher pressure caused by increasing the compression ratio that made the spray to break up faster .

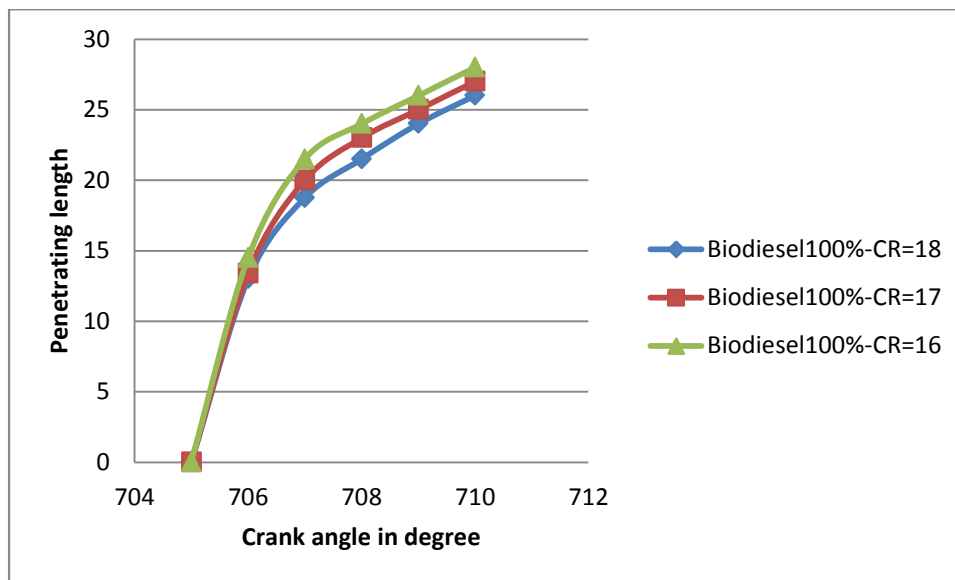


Figure 13: penetrating length of biodiesel blending ratio 100 % spray at different compression ratio.

#### 4. Conclusions

In this study a cold flow simulation was done to engine with compression ratio 18 and was validated against [1], then another two cold flow simulations were done to the engines with compression ratio 17 and 16 respectively, after that a diesel spray model was integrated to the engine with compression ratio 18 and the penetrating length was validated against [1]. Upon that, a spray models with Diesel and different biodiesel blending ratios 20%, 60% and 100% were integrated to the engines with compression ratios 18, 17 and 16 respectively, and it was concluded that:

1- Increasing engine compression ratio resulted in decreasing spray penetrating length that is because

as the compression ratio increased the ambient pressure increased causing the spray penetrating length to become shorter as it causes the spray to break up faster.

2- Increasing biodiesel blending ratio resulted in longer spray penetrating length that is because as biodiesel blending ratio increased the viscosity of the fuel increased causing an increase to spray penetrating length because of the higher inertia of fuel particles.

#### References:

[1] Mohamed Maher, Ahmed Abu-Elhamey, Omar Hassan, Alaa El-Din Ramadan, Aya Diab, Mostafa



Abdelkhalek, Adham Mohamed and Mohamed Abdel-Hay (2016). CFD Modeling of spray formation in Diesel engines. Athens Journal of Technology and Engineering.

[2] Jeong-Kuk Yeom and Woo-Sung Jung. (2015). Experimental and Numerical Analysis of Breakup Process of Biodiesel Fuel Spray. International Journal of Precision Engineering and Manufacturing, Vol. 16, No. 7, pp. (1279-1291).

[3] Mahmoud Yousefifard, Parviz Ghadimi and Hashem Nowruzi. (2015). Numerical Investigation of the effects of chamber Backpressure on the HFO Spray Characteristics .International Journal of Automotive Technology, Vol. 16, No. 2, pp. (339–349).

[4] Ahmed Abed Al-Kadhem Majhool, Abbas Alwi Sakhir ALJeebori. (2012) Study of Modeling Spray Penetration of Biodiesel Fuel under Transient Engine Conditions. Academic Research International , Vol. 3, No. 3, [www.journals.savap.org.pk](http://www.journals.savap.org.pk).

[5] Amir Khalid, Norrizam Jaat, Mohd Faisal Hushim, Bukhari Manshoor, Izzuddin Zaman, Azwan Sapit and Azahari Razali. (2017). Computational Fluid Dynamics Analysis of High Injection Pressure Blended Biodiesel. International Research and Innovation Summit.

[6] Hongzhan Xie, Lanbo Song, Yizhi Xie, Dong Pi, Chunyu Shao and Qizhao Li. ( 2015) .An Experimental Study on the Macroscopic Spray Characteristics of Biodiesel and Diesel in a Constant Volume Chamber. Energies, pages (5952-5972).[www.mdpi.com/journal/energies](http://www.mdpi.com/journal/energies).

[7] Belachew Tesfa, Rakesh Mishra, Fengshou Gu and Nicholas Powles. (2010).prediction models for density and viscosity of biodiesel and their effects on fuel supply system ci engines. Elsevier, renewable Energy35, pages (2752-2760).